Isomerization Processes of Electronically Excited Stilbene and Diphenylbutadiene in Liquids: Are They One-Dimensional?

Minyung Lee,[†] John N. Haseltine,[‡] Amos B. Smith III,* and Robin M. Hochstrasser*

Contribution from the Department of Chemistry, University of Pennsylvania, Philadelphia, Pennsylvania 19104. *Received September 26, 1988*

Abstract: Various "stiff" diphenylbutadienes with the phenyls held rigid by saturated chains of 2-4 carbons connecting the 2-position of phenyl to the polyene unit have been prepared, and their photophysics explored. The synthesis entailed a combination of Wittig reactions and the Wadsworth-Emmons modification. The temperature dependence of their fluorescence shows that the barriers to excited-state isomerism vary from 1.5 to 4.7 kcal mol^{-1}. The fluorescence lifetimes depend on viscosity, signifying that the barrier crossing is inhibited in more viscous solvents. The rotational reorientation times do not show a linear relation with viscosity. If the effective friction for barrier crossing is assumed to be proportional to that for overall rotation, the Kramers theory predicts the form of the friction dependence of the barrier crossing for all compounds studied. The marked deviations from a simple hydrodynamic interpretation of Kramers equation occur when the solvent size exceeds that of the solute.

Recently the Kramers' problem[1] of understanding barrier crossing processes of a Brownian particle influenced by solvent collision (friction) has drawn renewed attention. The stochastic dynamics is described by the Langevin equation involving an external force term or equivalently by a special form of the Fokker-Plank equation.[2,3] Computer experiments employing molecular dynamics simulations can be carried out to test the theory. Because of recent advances in picosecond spectroscopy, it is now possible to measure directly and precisely the rate constants for real chemical reaction systems. Among them are the photoisomerization of stilbene,[4-13] diphenylbutadiene (DPB)[7,8,14-18] and some dye molecules,[18,19] and the conformational change of binaphthyl,[20-22] bifluorene,[23] and anthracene analogues.[24]

The analytic solutions of the Fokker-Plank equation are obtained under the assumptions[1,2] that the process is one-dimensional and Markovian, the potential is piecewise parabolic, and the potential barrier is high enough so that a Boltzmann distribution is maintained in the reactant well. According to the Kramers equation, the barrier crossing rate could either increase or decrease as a function of the friction constant, depending on the coupling strength between the solute and solvent. By dividing the entire phase space into two parts, the inertial and diffusive regimes, a convenient description of the dynamic solvent effect acting on the reaction coordinate can be obtained. The inertial regime corresponds to the weak collision limit of gas-phase theories so that the energy diffusion (activation) may control the reaction. On the other hand, in the diffusive regime the spatial diffusion governs the barrier crossing process, and the rate becomes a monotonically decreasing function of the solvent friction. Therefore, it is expected that there should exist a "turnover" region connecting two regimes where the reaction rate reaches the maximum. Many theoretical studies have been concerned with the derivation of a single rate equation that describes the turnover region correctly, but the treatments are not yet far from the interpolation procedure of Kramers' solutions.[25-28] Kramers' model has been also extended to many dimensional and non-Markovian systems.[27-32]

In normal liquids it is expected that barrier crossing processes involving large molecules are diffusional. The one-dimensional Kramers' equation relevant to the isomerization process in this regime is given by

$$k_{nr} = \frac{\omega_a}{2\pi\omega_b}\frac{\beta}{2}\left\{\left[1+\left(\frac{2\omega_b}{\beta}\right)^2\right]^{1/2}-1\right\}\exp(-E_b/k_BT) \qquad (1)$$

where ω_a is the well frequency and ω_b is the barrier frequency. E_b is the barrier height. β is the angular velocity correlation frequency (the reduced friction constant), having the units of s^{-1}.

For Brownian motion β can be related to the solvent viscosity η via the Stokes-Einstein relation, assuming slip boundary conditions:

$$\beta = (4\pi dr^2/I) = \eta \qquad (2)$$

where I is the moment of inertia, d is the hydrodynamic radius, and r is the radius of gyration. The isomerization rates of *trans*-stilbene and DPB in *n*-alkane solvents have been extensively

[†] Present address: Department of Chemistry, University of California at Berkeley, Berkeley, CA 94720.
[‡] Present address: Department of Chemistry, Yale University, New Haven, CT 06511.

(1) Kramers, H. A. *Physica* **1940**, *7*, 284.
(2) Chandrasekhar, S. *Rev. Mod. Phys.* **1943**, *15*, 1.
(3) McCaskill, J. S.; Gilbert, R. G. *Chem. Phys.* **1979**, *44*, 389.
(4) Hochstrasser, R. M. *Pure Appl. Chem.* **1980**, *52*, 2683.
(5) Rothernberger, G.; Negus, D. K.; Hochstrasser, R. M. *J. Chem. Phys.* **1983**, *79*, 5360.
(6) Lee, M.; Holtom, G. R.; Hochstrasser, R. M. *Chem. Phys. Lett.* **1985**, *118*, 359.
(7) Lee, M.; Bain, A. J.; McCarthy, P. J.; Han, C. H.; Haseltine, J. N.; Smith III, A. B.; Hochstrasser, R. M. *J. Chem. Phys.* **1986**, *85*, 4341.
(8) Lee, M.; Hochstrasser, R. M. In *Ultrafast Phenomena V*; Fleming, G. R., Siegman, A. E., Eds.; Springer: Berlin, 1986.
(9) Maneke, G.; Schroeder, J.; Troe, J.; Voss, F. *Ber. Bunsen-Ges. Phys. Chem.* **1985**, *89*, 896.
(10) Sundstrom, V.; Gillbro, T. *Ber. Bunsen-Ges. Phys. Chem.* **1985**, *89*, 222.
(11) Courtney, S. H.; Fleming, G. R. *J. Chem. Phys.* **1985**, *83*, 215.
(12) Fleming, G. R.; Courtney, S. H.; Balk, M. W. *J. Stat. Phys.* **1986**, *42*, 83.
(13) Courtney, S. H.; Kim, S. K.; Canonica, S.; Gleming, G. R. *J. Chem. Soc., Faraday Trans. 2* **1986**, *82*, 2065.
(14) Velsko, S. P.; Fleming, G. R. *J. Chem. Phys.* **1982**, *76*, 3553.
(15) Keery, K.; Fleming, G. R. *Chem. Phys. Lett.* **1982**, *93*, 322.
(16) Courtney, S. H.; Fleming, G. R. *Chem. Phys. Lett.* **1984**, *103*, 443.
(17) Courtney, S. H.; Fleming, G. R.; Khundkar, L. R.; Zewail, A. H. *J. Chem. Phys.* **1984**, *80*, 4559.
(18) (a) Velsco, S. P.; Fleming, G. R. *Chem. Phys.* **1982**, *65*, 59. (b) Velsco, S. P.; Waldeck, D. H.; Fleming, G. R. *J. Chem. Phys.* **1983**, *78*, 249. (c) Kim, S. K.; Fleming, G. R. *J. Phys. Chem.* **1988**, *92*, 2168.
(19) Akesson, E.; Sundstrom, V.; Gilbro, T. *Chem. Phys.* **1986**, *106*, 269.
(20) Hochstrasser, R. M. *Can. J. Chem.* **1961**, *39*, 459.
(21) Jonkman, H. T.; Wiersma, D. A. *J. Chem. Phys.* **1984**, *81*, 1573.
(22) (a) Shank, C. V.; Ippen, E. P.; Teschke, O.; Eisenthal, K. B. *J. Chem. Phys.* **1977**, *69*, 5547. (b) Millar, D. P.; Eisenthal, K. B. *J. Chem. Phys.* **1985**, *83*, 5076. (c) Bowman, R. M.; Eisenthal, K. B.; Millar, D. P. *J. Chem. Phys.* **1988**, *89*, 762.
(23) Lee, M. Ph.D. Thesis, University of Pennsylvania, 1987.
(24) Flom, S. R.; Nagarajan, V.; Barbara, P. F. *J. Phys. Chem.* **1986**, *90*, 2085, 2092.
(25) Visscher, P. B. *Phys. Rev. B.* **1976**, *13*, 3272; **1976**, *14*, 347.
(26) Skinner, J. L.; Wolynes, P. G. *J. Chem. Phys.* **1978**, *72*, 2143.
(27) Grote, R. F.; Hynes, J. T. *J. Chem. Phys.* **1980**, *73*, 2715.
(28) Carmeli, B.; Nitzan, A. *J. Chem. Phys.* **1983**, *79*, 393.
(29) Zawadski, A. G.; Hynes, J. T. *Chem. Phys. Lett.* **1985**, *113*, 476.
(30) Straub, J. E.; Borkovec, M.; Berne, B. J. *J. Chem. Phys.* **1985**, *83*, 3172; **1986**, *84*, 1788.
(31) Bagchi, B.; Oxtoby, D. W. *J. Chem. Phys.* **1983**, *78*, 2735.
(32) Lee, S.; Karplus, M. *J. Phys. Chem.* **1988**, *92*, 1075.

0002-7863/89/1511-5044$01.50/0

Scheme I

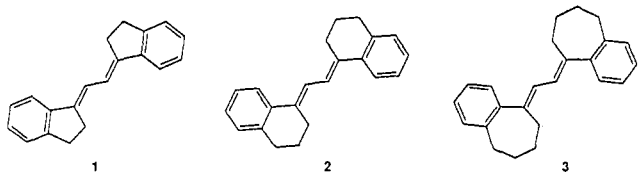

compared with the Kramers equation. The experimentally observed rates decreased much more slowly than the Kramers rates did when hydrodynamic variables (eq 2) were used to describe β. Several attempts to explain this discrepancy have been made: (i) The isomerization might be a multidimensional process.[5,14] (ii) The effect of frequency dependent friction may be operative in the viscosity range (0.2–3.5 cP), requiring the use of a generalized Langevin equation in Kramers theory.[31] (iii) Different solvents may alter the barrier, so the observed deviations are due to the solvent shifts.[9] (iv) The use of hydrodynamics may not be appropriate to the molecular system, because the solute and solvent sizes are comparable so that β cannot be obtained via eq 2.[7,13] Although ii and iv deal with the problem of the effective friction acting on the reaction coordinate, the physical origin for them is very different.

There were many efforts to find out solvent size effects on the overall rotational motion of solute using various picosecond spectroscopic techniques.[33] In ref 7 we therefore focused our attention on the validity of using hydrodynamic variables in the Kramers equation: The rotational reorientation times of *trans*-stilbene and stiff DPB in hydrocarbon solvents were measured and compared with a hydrodynamic equation (Stokes–Einstein–Debye equation (SED)). The rotational relaxation data deviated from the SED equation in the same solvent regime as the isomerization data deviated from the Kramers theory. These observations led us to suggest that it is the hydrodynamic variable that is inappropriate rather than Kramers model itself.[7] In other words, the macroscopic solvent viscosity is not a useful variable for the Kramers model whenever the molecular size of the solvent is comparable or larger than that of the solute. This notion has been supported by Ben-Amotz and Scott, who measured the overall rotational motion for many different molecular systems in which the relative size between solutes and solvents are different.[34]

To replace the Stokes–Einstein relation, a Hubbard relation[35] which relates rotational diffusion times, τ_R, to angular velocity correlation frequencies (AVCF), β_R, was used:

$$\beta_R = (6k_BT/I_R)\tau_R \qquad (3)$$

The Kramers–Hubbard fit was satisfactory and generated more physically reasonable barrier frequencies for stilbene than had been obtained with estimates of the frequency-dependent friction.[5] For *trans*-stilbene $\omega_a = 196$ cm^{-1} and $\omega_b = 176$ cm^{-1} were obtained. The assumption in this procedure is that rotational diffusion and torsional motion have linear responses to collision forces. The success of the Kramers–Hubbard approach eliminates the need for the explanation made by Troe and co-workers[9] that the deviation be entirely attributed to the solvent shifts, although in a final analysis such effects would surely need to be considered as well.

The goal of the present paper is to evaluate further the transferability of rotational relaxation parameters to the barrier crossing dynamics by studying three derivatives of DPB (stiff DPBs), designed such that the size of the isomerizing moieties was varied by changing the bridging ring size. The three systems were *E,E*-diindanylidenylethane (Scheme I, **1**, stiff 5-DPB), (*E,E*)-bis(tetrahydronaphthylidenyl)ethane (**2**, stiff 6-DPB), and *E,E*-bis(benzosuberanylidenyl)ethane (**3**, stiff 7-DPB). The photophysics of those molecules was also studied. In these experiments, a series of alkane solvents is used to avoid as much as possible changes of the barrier height due to solvent polarity. Nevertheless, the polarizability of those homologous solvents are slightly different, thereby introducing small effects on the potential surface. The dimensionality aspects in the isomerization of stilbene and DPB are also considered in this study.

Scheme II

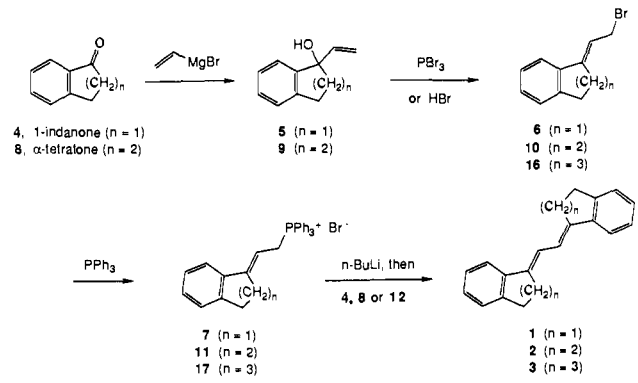

Scheme III

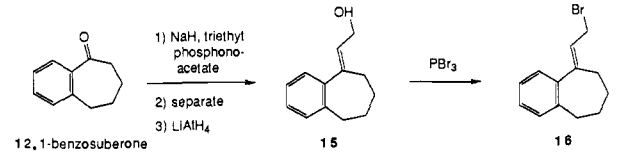

Results and Discussion

Preparative Experiments: Synthesis of Stiff Diphenylbutadienes. (*E,E*)-Diindanylidenylethane (**1**, $C_{20}H_{18}$, mp 190.5–192 °C) and (*E,E*)-bis(tetrahydronaphthylidenyl)ethane (**2**, $C_{22}H_{22}$, mp 144–146 °C) were prepared from commercially available 1-indanone (**4**) and α-tetralone (**8**), respectively, each in four steps as outlined in Scheme II.[36] Initially, vinyl Grignard addition supplied the corresponding tertiary alcohols, **5** and **9**.[37] Subsequent bromination by allylic nucleophilic substitution gave the primary *E*-allylic bromides, **6** and **10**. Alcohol **5** was particularly prone to acid-catalyzed elimination as an undesired side reaction, but its conversion to bromide **6** could be effected by the use of a less acidic reagent, phosphorus tribromide. The unstable bromides were immediately treated with triphenylphosphine to form the crystalline phosphonium salts. Wittig reaction between each salt and the corresponding starting ketones (**4** and **8**, respectively) then provided the *E,E*-dienes, **1** and **2**, which crystallized conveniently from the product mixtures.

(*E,E*)-Bis(benzosuberanylidenyl)ethane (**3**, $C_{24}H_{26}$, mp 186.5–187.5 °C) was accessible by a slightly different route starting from 1-benzosuberone (**12**).[36] Olefination of this ketone by the Wadsworth–Emmons modified Wittig reaction as illustrated in Scheme III gave a chromatographically separable mixture of geometrically isomeric unsaturated esters. Reduction of the *E* isomer to allylic alcohol **15** with lithium aluminum hydride was followed by treatment with phosphorus tribromide, to provide the *E*-allylic bromide (**16**). Completion of the synthesis of **3** then proceeded as outlined above.

That each of the dienes (**1**, **2**, and **3**) was in fact a single isomer possessing a C_2 axis of symmetry was evident from their ^{1}H and ^{13}C NMR spectra. X-ray diffraction structure analyses confirmed the olefin geometries as being of the *E,E* configuration.[38]

Photophysics of Stiff DPB. The steady-state absorption and emission spectra for three stiff DPBs in the singlet excited state (S_1) region are shown in Figures 1 and 2, respectively. The spectrum of stiff 5-DPB is structured, with peak positions very

(33) Chang, T. J.; Eisenthal, K. B. *Chem. Phys. Lett.* **1971**, *11*, 368. Rice, S. A.; Kenny-Wallace, G. A. *Chem. Phys.* **1980**, *47*, 161. Waldeck, D. H.; Fleming, G. R. *J. Phys. Chem.* **1981**, *85*, 2614. Philips, J. A.; Webb, S. P.; Clark, J. H. *J. Chem. Phys.* **1985**, *83*, 5810.
(34) Ben-Amotz, D.; Scott, T. W. *J. Chem. Phys.* **1987**, *87*, 3739.
(35) Hubbard, P. S. *Phys. Rev.* **1963**, *131*, 1155.
(36) Aldrich Chemical Company, Milwaukee, WI.
(37) Marcou, A.; Normant, H. *Bull. Soc. Chim. Fr.* **1965**, 3491.
(38) Carroll, P. J.; Haseltine, J. N.; Hochstrasser, R. M.; Smith, A. B., III *Acta Crystallogr.*, in press.

Table I. Fluorescence Lifetimes of *trans*-DPB and Stiff DPBs (picoseconds)

solvent	*trans*-DPB[a]	stiff 5-DPB	χ^2	stiff 6-DPB	χ^2	stiff 7-DPB	χ^2
n-pentane	450	366	1.56	54	1.09	10	3.0
n-hexane	485	406		70	1.06		
n-heptane		453	2.10	88	1.29		
n-octane	580	520	1.91	109	1.01		
n-nonane		565	2.01	131	0.97		
n-decane	630	594	1.62	155	1.27		
n-undecane	690	632	1.62	174	1.02		
n-dodecane	710	670	1.85	203	1.13		
n-tridecane		695		230	1.00		
n-tetradecane	740	715	2.7	261	1.00		
n-pentadecane	755	738	1.6	288	1.16		
n-hexadecane		765	2.27	314	1.21	50 (?)	

[a] Reference 14 (no χ^2 given).

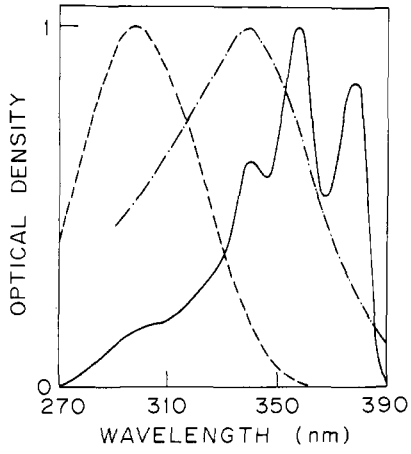

Figure 1. Absorption spectra of stiff DPB path length 1 cm: stiff 5-DPB (—) 1.62×10^{-5} M; stiff 6-DPB (-·-) 2.55×10^{-5} M; stiff 7-DPB (--) 3.37×10^{-5} M.

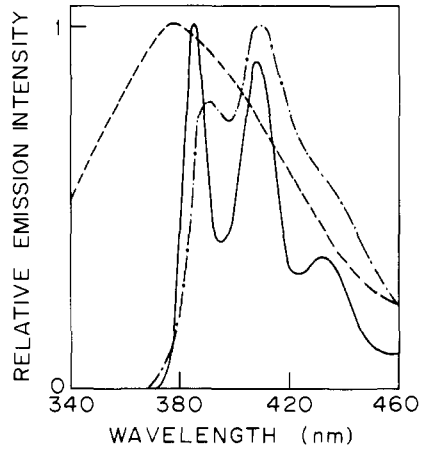

Figure 2. Emission spectra of stiff DPB.

similar to those of *trans*-DPB.[39] The absorption spectrum of stiff 6-DPB is blue shifted to 340 nm and unstructured, while the emission spectrum is structured. The absorption spectrum of stiff 7-DPB is even further blue shifted (maximum at 300 nm), and both absorption and emission spectra are unstructured. These facts indicate that the structural alterations (stiffening) may affect the S_0 and S_1 states significantly.

Photophysics. Table I shows the lifetime data for *trans*-DPB and stiff DPBs. A striking feature is that the introduction of strain into the bridging ring between the rings and diene (referred to as stiffening) shortens the excited-state lifetimes. A lifetime shortening due to stiffening was also observed for the stilbene molecule and attributed to changing the excited potential surface.[5] To check whether or not this is the case for diphenylbutadiene,

(39) Bennet, J. A.; Birge, R. *J. Chem. Phys.* **1980**, *73*, 4234.

Table II. Photophysical Properties of *trans*-Stilbene, *trans*-DPB, and Their Stiffened Molecules

molecule	$10^8 k_r$, s^{-1}	E_b, kcal/mol
trans-stilbene	3.7	3.5
stiff 5-stilbene	4.6	1.5
trans-DPB	7.7	4.7
stiff 5-DPB	7.1	4.7
stiff 6-DPB	6.2	3.3

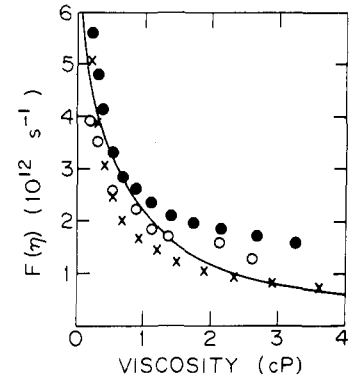

Figure 3. Frequency factor vs solvent shear viscosity. The solid curve is the nonlinear least-squares fit (SIMPLEX) of the hydrodynamic Kramers equation to data. For molecular parameters, see ref 7. ○, *trans*-DPB; ⊙, stiff 5-DPB; ×, stiff 6-DPB.

the potential barriers (E_b) and radiative rate constants (k_r) of stiff 5-DPB were measured: They are compiled in Table II with previously reported data for other diphenylpolyenes.[7,14,40-42] Compared with stilbene, the effect of stiffening on the k_r and E_b of DPB is less dramatic. The potential barriers for *trans*-DPB and stiff 5-DPB are virtually identical, while that of stiff 6-DPB is significantly smaller. The lifetimes of stiff 7-DPB are even shorter than stiff 6-DPB, so that the E_b of stiff 7-DPB is apparently smaller than other DPBs. The nonradiative decay rate constant k_{nr} is obtained from lifetime data by using the relation

$$k_{nr} = 1/\tau_F - k_r \quad (4)$$

It is assumed that a barrier crossing process (isomerization) is the major channel for the nonradiative decay. The barrier heights for DPB derivatives are different, so it is necessary to plot the isomerization data in terms of the frequency factor, $F = k_{nr} \exp(E_b/k_B T)$. Figure 3 shows the variation of the frequency factor with viscosity. Considering the large difference in the potential barriers (4.7 kcal/mol for *trans*-DPB and stiff 5-DPB, and 3.3 kcal/mol for stiff 6-DPB), the data give, in large measure, the same curvature, and the form of the F factor is not obviously correlated to the size of the molecule. This indicates that the

(40) Saltiel, J.; D'Agostino, J. T. *J. Am. Chem. Soc.* **1972**, *94*, 6445.
(41) Sumitani, M.; Nakashima, N.; Yoshihara, K.; Nakagura, S. *Chem. Phys. Lett.* **1977**, *51*, 183.
(42) Syage, J. A.; Lambert, W. R.; Felker, P. M.; Zewail, A. H.; Hochstrasser, R. M. *Chem. Phys. Lett.* **1982**, *88*, 266.

Table III. Rotational Orientational Time and Angular Velocity Correlation Frequency Calculated by the Hubbard Relation

	trans-stilbene		stiff 6-DPB[b]	
solvent	τ_R, ps	$10^{13}\beta$	τR (ps)	$10^{13}\beta$
n-pentane	12	0.89	26	0.95
n-hexane	16	1.18	31 ± 2	1.13
n-heptane	19	1.34	35 ± 3	1.28
n-octane	25	1.8	43 ± 3	1.6
n-nonane	27	1.97	56 ± 3	2.08
n-decane	32	2.28	61 ± 2	2.24
n-undecane	50 ± 4	3.21	73 ± 7	2.7
n-dodecane	54	3.59	86 ± 2	3.17
n-tridecane	58	4.18	95 ± 2	3.5
n-tetradecane	65	4.69	112 ± 4	4.13
n-pentadecane	72	5.16	128 ± 5	4.72
n-hexadecane	82 ± 7	5.88	132 ± 6	4.88

[a] 22 °C. [b] 19 °C.

stiffening size, which affects the moment of inertia of the moving parts, may not change the shape of the potential significantly even though the potential barrier is altered. This means that the effective well and barrier frequencies of the stiff DPBs should be similar to those of *trans*-DPB.

In Figure 3 the solid curve is a nonlinear least-squares fit to the data using Kramers equation with hydrodynamic variables. In spite of the fact that the data are scattered, the fit is poor. That is, the hydrodynamic Kramers equation does not correctly predict the proper curvature of the experimental data.

Kramers–Hubbard Approach. It was demonstrated[7] that the failure of eq 1 to reproduce the isomerization data for *trans*-stilbene and a stiff 6-DPB in *n*-alkanes is due to using a simple Stokes–Einstein relation to calculate the value of β. The solvent-influenced reaction dynamics is more complex than this if the size of solutes and solvents are comparable. The use of the Hubbard relation, as previously employed[7] is an alternative approach for this problem. Table III shows the rotational reorientation times, τ_R, and angular velocity correlation frequencies, β, obtained via eq 3.[7] The measured τ_R values refer to the end-over-end tumbling motion, because the transition dipole moments for both stilbene and DPB in the singlet excited state are mainly along the longest molecular axes. We should expect that for solvents whose component molecules are small enough the τ_R of stilbene and DPB be similar. Indeed the τ_R data are almost identical for these two solutes in *n*-pentane to *n*-decane but are significantly different for paraffins longer than *n*-undecane.

In Figure 4, the frequency factors, F, are plotted as a function of β_R, and the solid curve is the Kramers–Hubbard fit to the data. Here we assumed that the AVCF for isomerization (β_i) is proportional to that for overall rotation (β_R):[7]

$$\beta_i = p\beta_R \tag{5}$$

where the proportionality factor p was introduced to accommodate the possible differences in the effectiveness of collisions in the isomerization and overall rotation process. The Kramers–Hubbard fit produces a much improved fit to the curvature of the experimental data. The obtained well and barrier frequencies as fitting parameters are 424 and 21 cm^{-1} (strictly $\omega_b = 21p$ cm^{-1}), respectively. When compared with the fit to stiff 6-DPB, the well frequency does not change, and if $p = 1$ the barrier frequency would be increased, making the curvature flatter.

At this point the coupling between internal motion and overall rotation requires consideration. In general a change in the internal (isomerism) coordinate is accompanied by a change in the moment of inertia for the overall motion so that the decoupling approximation requires to be justified. This is an old problem for NMR relaxation time measurements.[43] Evans and co-workers extensively studied this matter[44] for *n*-butane and stilbene isomerization

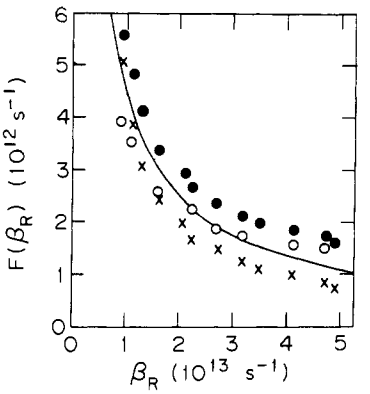

Figure 4. Frequency factor vs the angular velocity correlation frequency; the solid curve is the nonlinear least-squares fit to the data. Symbols are the same as in Figure 3.

employing a diffusion equation in four variables (the three Euler angles for the overall rotation and a torsional angle for the internal motion). Unlike NMR relaxation data, where the decoupling is a necessary assumption to analyze the data, the picosecond fluorescence and anisotropy measure these motions independently. Furthermore, the overall rotational correlation times for stilbene are many times faster than the isomerization times in most solvents. Therefore, it is suggested that the coupling between the overall and the internal angular momenta may be neglected on the experimental time scales.

The Kramers–Hubbard approach is an attempt to understand the chemical reaction dynamics at a molecular level. There have been many efforts to characterize potential surfaces for molecular systems by fitting data to the Kramers equation with hydrodynamic variables. Because of the apparent success of the Kramers–Hubbard approach, it is useful to consider some of the previous measurements on solvent-influenced reaction dynamics from that standpoint. A demonstrated earlier[5,7,13] when solvent and solute molecules have a comparable size, the macroscopic solvent viscosity cannot be used as the exact measure for the friction. To focus on the nonpolar frictional influences, we confine our discussion to nonpolar molecules and exclude the results for (dimethylamino)benzonitrile,[45] DODCI[18] (for which a Kramers–Hubbard approach was found not to work[18]), its analogue,[19] and more polar stilbenes.[46]

The internal motion of binaphthyl occurs around a single carbon–carbon bond, and the moving parts are rigid so that it has been thought the dynamics may be closely one-dimensional. This molecule has been subjected to many experimental[20-22] and theoretical studies.[3,47] In the excited state, an appreciable barrier (460 cm^{-1}) exists for the conformational change in the condensed phase.[20] A viscosity dependence for the motion was observed in some nonpolar solvents and a series of normal alcohols and the Kramers fit, incorporating hydrodynamic variables, was successfully applied to the data.[3,22] However the *n*-alkane data[22c] required an effective friction based on the overall rotational correlation function to fit to a Kramers function.[22c] The potential barrier ($1.5k_BT$) in this case at room temperature seems too low for Kramers theory to be applicable: In the case of stiff stilbene[5] the low barrier appeared to cause the observed linear relation between lifetime and viscosity. The internal motions of alkenes bonded to anthracenes in a series of *n*-alkane solvents were studied by Barbara and co-workers employing picosecond spectroscopy.[24] Like binaphthyl, the conformational change of this molecule involves a rotation about a carbon–carbon single bond so that the effective dimensionality may be low. However, relatively small molecular volume changes accompany the motion so the friction

(43) Woessner, D. E. *J. Chem. Phys.* **1962**, *37*, 647; **1965**, *42*, 1855.
(44) Evans, G. T. *J. Chem. Phys.* **1980**, *72*, 3849. Evans, G. T.; Knauss, D. C. *J. Chem. Phys.* **1980**, *72*, 1504; **1981**, *75*, 4647. Ladanyi, B. M.; Evans, G. T. *J. Chem. Phys.* **1983**, *79*, 944.
(45) Hicks, J.; Vandersall, M.; Babarogic, Z.; Eisenthal, K. *Chem. Phys. Lett.* **1985**, *116*, 18. Hicks, J. M.; Vandersall, M. T.; Sitzmann, E. V.; Eisenthal, K. B. *Chem. Phys. Lett.* **1987**, *135*, 413.
(46) Zeglinski, D. M.; Waldeck, D. H. *J. Phys. Chem.* **1988**, *92*, 692.
(47) Riley, M. J.; Lacey, A. R.; Sceats, M. G.; Gilbert, R. G. *Chem. Phys.* **1982**, *72*, 83.

due to solvent size or inertial effects is expected to be pronounced for these model systems. The Kramers–Hubbard approach has now been successfully applied to this molecular system.[48] A similar approach to that used in our work was used recently for stilbene in alkanes[18c] and dimethoxystilbene.[46] The alkane studies[18c] incorporated data at viscosities intermediate between those of the alkanes by varying the temperature. The resulting fit to Kramers equation was unsatisfactory.

The isomerization of *n*-butane has been studied only by theoretical molecular dynamics simulations. The torsional amplitude of the methyl group is comparable with that of the alkenyls in alkenylanthracenes. Therefore, it would not be surprising if the hydrodynamic Kramers equation were also inapplicable to *n*-butane in most liquid solvents.[49]

Another example is the chair–boat isomerization of cyclohexane.[50] The isomerization reaction involves the small-amplitude motion of one carbon atom (CH_2), which might have significant inertial content. In other words, the motion might be closer to Lorentzian rather than Brownian.[51] On these grounds the use of the Stokes–Einstein relation for cyclohexane isomerization might omit some of the important motions. The ultraviolet fluorescence up-conversion gating measurements on the rotational motion of aniline by Myers et al.[52] provided experimental evidence for nondiffusive, inertial-like rotational motion whose time scale is comparable with the free rotor correlation time. Similar effects might occur in the isomerisms of the molecule $(\pi\text{-}C_5H_5)Rh(C_2H_4)_2$, in which the barrier crossing process involves ethylenes.[53] These systems are more properly dealt with using the BGK model.[54]

Excited-State Potential Surface. An important goal of applying stochastic models to the isomerization data is to identify the excited potential surface on which the dynamics occurs. The outcome of the Kramers fit is the vibration frequency in the initial well and the barrier frequency. To understand the excited-state potential along the reaction coordinate for diphenyl polyenes, their singlet electronic states must be fully understood. They each have two low-lying electronic states, A_g and B_u.[55] For long-chain polyenes with $n > 2$, the A_g state lies below the B_u state. Since transitions between the A_g excited state and the ground state are relatively weak, it is expected that the degree of mixing of A_g and B_u excited states will determine the radiative properties of the electronically excited molecules. Indeed, the radiative decay rate constants of such polyenes in solution critically depend on the solvent polarizability,[56] which also must affect the energy gap between the two states. On the other hand, the lowest excited state of *trans*-stilbene is a B_u type state, so the radiative rate constant of the molecule is almost independent of solvents.[57] The theoretical and experimental evidence indicates that an avoided crossing of the B_u state with the higher A_g state forms the excited-state potential surface for the stilbene molecule.[58] The position of the initial well in the solution phase may not be exactly at 0° due to the repulsive interaction of phenyl ring with the ethylenic hydrogens. The angular location of the barrier maximum is unknown. The well frequency and the barrier frequency are known qualitatively from solution and gas-phase experiments. The lifetime measurements of the molecule in high-pressure ethane set the minimum well frequency at 160 cm^{-1}.[6] The Kramers–Hubbard approach to the problem requires values of ω_a = 196 cm^{-1} and ω_b = 176 cm^{-1}. These values were obtained assuming the partition function ratio for the reactant and the transition state and the proportionality factor p are unity. The same conclusion was independently made by Fleming and co-workers.[13] Their Kramers–Hubbard fit for *trans*-stilbene in *n*-alkane solvents gave ω_a = 193 cm^{-1} and ω_b = 182 cm^{-1}.

The excited states of diphenylbutadiene ($n = 2$) are not fully understood yet. By using two-photon spectroscopy, it has been claimed that the S_1 state is of A_g symmetry in liquid solutions[59] and in glassy solution.[60] A recent supersonic jet study by Zewail and co-workers showed that in the isolated DPB molecule the lowest state is of A_g symmetry.[61] Velsko and Fleming[14] argued that similarity of the radiative properties of DPB and stilbene in liquids suggests that in both cases the emitting state must be B_u. They proposed that an avoided crossing of a B_u state with an A_g of DPB state gives rise to the potential barrier of 1650 cm^{-1}. It should be noted that the barrier for jet-cooled DPB is significantly lower (1050 cm^{-1}).[61] These two results are reconciled by invoking a solvent-assisted electronic level inversion.[62] A time-resolved resonance Raman study[63] suggested that the lowest singlet state of DPB in liquids is B_u, supporting the emission spectroscopy measurements. As first proposed by Velsko and Fleming,[14] it seems likely that the excited-state potential of DPB in solution is formed in a way similar to that of *trans*-stilbenes.

Concerning One-Dimensionality. There have been speculations about the effective dimensionality for stilbene and diphenylbutadiene isomerization. To address this question, it is important to find out which vibrational frequency best describes the reactive mode responsible for the isomerization. The lifetime measurements for stilbene in supercritical fluid ethane showed that the well frequency should be greater than or equal to 160 cm^{-1}. The Kramers–Hubbard fit to the stilbene data (see above) gave a well frequency of 196 cm^{-1} with the foregoing assumptions. Among 72 vibrational normal modes of *trans*-stilbene, the ν_{25} mode having frequency of 198 cm^{-1} is closest to those numbers.[64] In fact the spectroscopic study of jet-cooled stilbene showed that only the ν_{25} mode (C_e–C_e–Ph symmetric in-plane bending mode) forms a long progression in both emission and absorption, while all the other modes undergo relatively little distortion upon excitation to S_1.[64c]

If it is assumed that the reactive motion contains a significant ν_{25} contribution, there are four other modes in stilbene with lower frequencies, and they are expected to be coupled to the reactive mode. The strength of coupling would then determine the dimensionality of the isomerization process: If the coupling were weak, the isomerization process could be regarded as one-dimensional.

Recently Berne et al. performed molecular dynamics simulations on a many-dimensional Langevin equation in which the reactive mode is linearly coupled to a nonreactive mode.[30] In the inertial regime the rate increased as $(E_b/k_BT)^{s-1}$, where s is the dimensionality as expected by the Hinshelwood–Kassel type theory. In the diffusive regime, however, the rate constant was essentially independent of dimensionality. Langevin dynamics becomes more complex for the nonlinearly coupled system,[65,66] but the molecular dynamics simulation gives almost the same results as with the linearly coupled system.[67] In addition, competition between the

(48) Barbara, P. F.; Walker, G. C. Ultrafast Measurements on Excited State Isomerization, a preprint.
(49) Rosenberg, R. O.; Berne, B. J.; Chandler, D. *Chem. Phys. Lett.* **1980**, *75*, 162. Rebertus, D. W.; Berne, B. J.; Chandler, D. *J. Chem. Phys.* **1979**, *70*, 3395.
(50) Hasha, D. L.; Eguchi, T.; Jonas, J. *J. Chem. Phys.* **1981**, *75*, 1571; *J. Am. Chem. Soc.* **1982**, *104*, 2290.
(51) Berne, B. J.; Skinner, J. L.; Wolynes, P. G. *J. Chem. Phys.* **1980**, *73*, 4314.
(52) Myers, A. B.; Pereira, M. A.; Holt, P. L.; Hochstrasser, R. M. *J. Chem. Phys.* **1987**, *86*, 5146.
(53) Xie, C.-L.; Campbell, D.; Jonas, J. *J. Chem. Phys.* **1988**, *88*, 3396.
(54) (a) Montgomery, Jr., J. A.; Chandler, D.; Berne, B. J. *J. Chem. Phys.* **1979**, *70*, 4056. (b) Kuharski, R. A.; Chandler, D.; Rabii, F.; Montgomery, Jr., J.; Singer, S. J. *J. Phys. Chem.*, in press.
(55) Huddson, B. S.; Kohler, B. E.; Schulten, K. In *Excited states*, Lim, E. C., Ed.; Academic Press: New York, 1982.
(56) Birks, J. B.; Tripathi, G. N. R.; Lumb, M. D. *Chem. Phys.* **1978**, *33*, 185.
(57) Sumitani, M.; Nakashima, N.; Yoshihana, K.; Nagakuna, S. *Chem. Phys. Lett.* **1977**, *51*, 183.
(58) Orlandi, G.; Siebrand, W. *Chem. Phys. Lett.* **1975**, *30*, 352.
(59) Swofford, R. L.; McClain, W. M. *J. Chem. Phys.* **1973**, *59*, 5740.
(60) Bennet, J. A.; Birge, R. R. *J. Chem. Phys.* **1980**, *73*, 4234.
(61) Shepanski, J. F.; Keelan, B. W.; Zewail, A. H. *Chem. Phys. Lett.* **1983**, *103*, 9.
(62) Rulliere, C.; Declemy, A.; Kottis, Ph. *Laser Chem.* **1985**, *5*, 185.
(63) Gustafson, T. L.; Palmer, J. F.; Roberts, D. M. *Chem. Phys. Lett.* **1986**, *127*, 505.
(64) (a) Warshel, A. *J. Chem. Phys.* **1975**, *62*, 214. (b) Zwier, T. S.; Carrasquillo, E.; Levy, M.; Levy, D. H. *J. Chem. Phys.* **1983**, *78*, 5493. (c) Scherer, N. F.; Shepanski, J.; Zewail, A. H. **1984**, *81*, 2181.
(65) Carmeli, B.; Nitzan, A. *Chem. Phys. Lett.* **1984**, *106*, 329.
(66) Agmon, N.; Kosloff, R. *J. Phys. Chem.* **1987**, *91*, 1988.

intramolecular vibrational redistribution (IVR) and intermolecular vibrational relaxation process can be a factor. That is, in liquids, the intermolecular relaxation whose time scale is the order of collisions might be faster than IVR for some motions, which means the effective dimensionality in liquids can be different than in gases.

Realistically *trans*-stilbene and DPB isomerization can involve at least two internal motions: The torsional motion around the double bond, which is responsible for the isomerization and the phenyl ring rotation. If the phenyl ring motion is blocked, then the stilbene dynamics becomes more likely one-dimensional. When the stiff stilbene data were compared with the Kramers model, Smoluchowski behavior (rate of isomerization proportional to viscosity) was observed,[5] which might indicate that the stiff stilbene is more likely one-dimensional than *trans*-stilbene. Agmon and Kosloff[66] treated this problem theoretically by solving a time-dependent diffusion equation involving a two-dimensional potential surface and obtained qualitative agreement with this experiment. However, stiffening of *trans*-stilbene reduces the potential barrier to only 2.5 k_BT at room temperature, which renders those interpretations less conclusive.

Stiff 5-DPB and stiff 6-DPB have potential barriers of 4.7 and 3.3 kcal/mol, respectively, which fulfill the assumption required in Kramers model. Our experimental data show that those molecules do not follow either the Kramers theory or its Smoluchowski limit. It is now clear that the deviation in the high friction regime is due not to multidimensionality but to the solvent size effects. As demonstrated in ref 7 and in this paper, the one-dimensional Kramers theory works well for these types of molecules when effective frictional constants are used.

The multidimensionality is very important to understand the so-called "Kramers turnover" region: higher dimensionality shifts the turnover to the lower friction regime. Molecular dynamics simulation studies on *n*-butane and cyclohexane[52] and experimental studies on cyclohexane[50] showed that the turnover region occurs in liquids. However, as pointed out in subsection B, these isomerization processes involve small amplitude and mass motion so that a quantitative agreement with the Kramers theory would be surprising. A gas-phase NMR study on cyclohexane demonstrated that the high-pressure limit is reached at 2–3 atm of gas pressure,[68] and so the observation of the turnover region in liquids has been questioned.[69] However, a recent molecular dynamics study still supports the liquid-phase measurement.[54b]

The isomerization rate of *trans*-stilbene in supercritical fluid ethane measured by Lee et al.[6] showed the turnover at a viscosity of 0.03 cP. This viscosity corresponds to the region between gas and conventional liquid. The occurrence of a turnover in this region was correctly predicted by Zawadski and Hynes,[70] who used a one-dimensional potential function with 4–6 vibrational degrees of freedom coupled to the reaction coordinate. However, the average vibrational energy for *trans*-stilbene is ca. 1800 cm^{-1} at room temperature, which is significantly higher than the barrier height (1200 cm^{-1}). Thus the role of collisions might be just to redistribute this internal energy rather than to activate molecules. Until this paradox[71] is resolved, the observation of a turnover region for the stilbene isomerization in the friction regime of 0.03 cP does not establish a multidimensional barrier crossing.

Concluding Remarks

To clarify some issues raised recently in the course of studying stochastic dynamics in the condensed phase, several stiff diphenylbutadienes were synthesized. Steady-state spectra, fluorescence lifetimes, and anisotropies of the molecules were measured by a picosecond single-photon-counting method having 10-ps resolution and compared with previously reported *trans*-stilbene, stiff stilbene, and *trans*-diphenylbutadiene data. The absorption and emission spectra and the radiative decay constant of stiff 5-DPB are similar to those for *trans*-DPB. Also the fluorescence lifetimes and the potential barrier for the nonradiative decay in alkane solvents are almost identical with *trans*-DPB, indicating that the five-membered stiffening does not significantly influence the excited-state potential surface. The photophysics of stiff 6-DPB are different from *trans*-DPB and stiff 5-DPB, so that in this case strain may affect the excited-state potential. The fluorescence lifetime was shorter and the barrier height was 3.3 kcal/mol, significantly lower than that of *trans*-DPB and stiff 5-DPB (E_b = 4.7 kcal/mol). The lifetimes of stiff 7-DPB were too short to measure accurately with the detection system employed in this work, probably as a result of a significantly lower barrier to isomerization.

The isomerization rates of stiff 5- and stiff 6-DPB in alkanes were compared with stochastic theories. They deviate from Kramers model when the Stokes–Einstein relation is employed. The Kramers–Hubbard fit correctly predicts the experimental curvature of isomerization rate versus friction for *trans*-stilbene, stiff 5-DPB, and stiff 6-DPB. This indicates that a solvent size effect dominates the deviations from Kramers theories that are obtained when the mascroscopic viscosity is used as a measure of the friction. We suggest that, in this context, an effective friction must be considered whenever the solvent molecules become comparable or larger than the solute.

We conclude that the stilbene and DPB isomerization can be effectively one-dimensional in the liquid state, because the Kramers–Hubbard fit, using angular velocity correlation frequencies adjusted to those needed to describe the overall rotation, give reasonable agreement with experiment and the Kramers turnover region occurs in the high-pressure fluid (100 atm). In other words, the barrier crossing seems to occur along a one-dimensional potential surface perhaps with coupling of a few nonreactive modes to the reactive mode. This leaves stilbene and diphenylbutadiene as good model systems with which to test stochastic statistical mechanical theories.

Experimental Details

Materials and Methods. Reactions were carried out under an argon atmosphere using dry, freshly distilled solvents, under anhydrous conditions in oven-dried glassware, unless otherwise noted. Diethyl ether and tetrahydrofuran (THF) were distilled under nitrogen from sodium/benzophenone; benzene was distilled from calcium hydride. *n*-Butyllithium was purchased from Aldrich Chemical Co. and standardized by titration with diphenylacetic acid. Solutions were dried over magnesium sulfate.

All reactions were monitored by thin-layer chromatography (TLC); flash column chromatography was performed with the solvents indicated using silica gel-60 (particle size 0.040–0.063 mm). Yields refer to chromatographically and spectroscopically pure compounds unless otherwise stated. Melting points were obtained on a Bristoline heated-stage microscope and are corrected. The IR and ^1H NMR spectra were obtained for $CHCl_3$ and $CDCl_3$ solutions, respectively. Proton and carbon-13 NMR spectra are reported as δ values relative to tetramethylsilane.

Samples of the stiff DPBs and *trans*-DPB were zone-refined before use, and the best solvents available were used.

The time-correlated single-photon-counting system to measure the fluorescence lifetimes (τ_F) and anisotropy decay times (τ_R) of stiff DPB was described elsewhere.[7] The instrument response function was 50 ps. The fluorescence lifetimes were temperature dependent and the values of the Arrhenius energy (at constant viscosity) were assumed to correspond to barrier heights (E_b) mentioned in the text.

1-Vinyl-1-indanol (5).[37] A solution of 1-indanone (**4**, 11.72 g, 88.68 mmol) in 25 mL of benzene was added dropwise over 30 min to a solution of vinylmagnesium bromide (175 mL, 1.0 M in THF, 170 mmol) in 150 mL of benzene. The reaction was stirred for 17 h, after which extractive aqueous workup gave a yellow oil. Flash column chromatography (hexanes:EtOAc, 23:2) provided the pure *alcohol* (12.67 g, 89%) as a colorless oil: IR ($CHCl_3$) 3600 (m), 3600–3300 (w), 3015 (s), 2950 (m), 1480 (m) 1460 (m) 995 (m), 930 (s) cm^{-1}; ^1H NMR (250 MHz, $CDCl_3$) δ 1.91 (br s, 1 H), 2.19 (ddd, J = 5.3, 7.9, 13.2 Hz, 1 H), 2.33 (ddd, J = 6.3, 7.9, 13.2 Hz, 1 H), 2.84 (ddd, J = 5.3, 8.0, 15.9 Hz, 1 H), 3.08 (ddd, J = 6.4, 7.8, 15.9 Hz, 1 H), 5.17 (dd, J = 1.4, 10.6 Hz, 1 H), 5.29

(67) Straub, J. E.; Borkovec, M.; Berne, B. J. *J. Chem. Phys.* **1987**, *86*, 4296.
(68) Ross, B. D.; True, N. S. *J. Am. Chem. Soc.* **1983**, *105*, 4871.
(69) Zawadzki, A. G.; Hynes, J. T. *Chem. Phys. Lett.* **1985**, *113*, 476. Hynes, J. T. *J. Stat. Phys.* **1986**, *42*, 149.
(70) Zawadzki, A. G.; Hynes, J. T., a preprint.
(71) We are indebted to Prof. G. R. Fleming for a valuable discussion on this point.

(dd, J = 1.4, 17.2 Hz, 1 H), 6.11 (dd, J = 10.6, 17.2 Hz, 1 H), 7.23–7.28 (comp m, 4 H); chemical ionization mass spectrum, m/e 160.0889 (M^+ calcd for $C_{11}H_{12}O$, 160.0888).

(*E*)-(2-Indanylidenylethyl)triphenylphosphonium Bromide (7). Phosphorus tribromide (0.74 mL, 7.9 mmol) was added dropwise to a stirred solution of alcohol **5** (3.00 g, 18.7 mmol) in 75 mL of diethyl ether at −20 °C over 3 min. The reaction was stirred at −20 °C for 10 min and then quenched by rapid addition of excess saturated sodium bicarbonate solution while stirring vigorously. Extraction of the mixture with ether, washing of the combined extracts with brine, and drying over magnesium sulfate gave a colorless solution. This was concentrated under reduced pressure to approximately 25 mL, then 50 mL of benzene was added, and concentration was resumed until the final volume was approximately 50 mL. Propene oxide (0.75 mL, 11 mmol) was added to the solution, and after cooling to 5 °C, triphenylphosphine (5.89 g, 22.5 mmol) was added with stirring. The solution was quickly warmed to approximately 20 °C and allowed to stand at room temperature for 2.5 h. The supernatant was removed, and the product washed with benzene (3 × 3.5 mL). Drying in vacuo provided the *salt* (**7**) as colorless crystals (2.52 g, 28%): mp 201.5–203 °C; IR ($CHCl_3$) 2940 (s), 1440 (s), 1240 (m), 1115 (s), 995 (w), 715 (m), 685 (s), 655 (s) cm^{-1}; ^1H NMR (250 MHz, $CDCl_3$) δ 2.35–2.37 (m, 2 H), 2.71–2.76 (m, 2 H), 4.79 (dd, J = 7.9, 15.1 Hz, 2 H), 5.77 (m, 1 H), 7.09–7.31 (comp m, 4 H), 7.65–7.92 (comp m, 15 H); chemical ionization mass spectrum, m/e 405.1725 (M^+ − Br calcd for $C_{29}H_{26}P$, 405.1772).

(*E*,*E*)-Diindanylidenylethane (1). *n*-Butyllithium (3.44 mL, 2.40 M in hexanes, 8.26 mmol) was added to a suspension of phosphonium salt **7** (4.01 g, 8.26 mmol) in 40 mL of THF at room temperature under argon until a faint yellow color persisted, and a further 3.44 mL (8.26 mmol) was added. The resulting suspension was stirred for 30 min, after which a solution of 1-indanone (**4**, 1.20 g, 9.09 mmol) in 5 mL of THF was added. The reaction mixture was heated to reflux for 4 h, then allowed to cool, poured into water, and extracted with methylene chloride. The combined extracts were washed with brine, dried over magnesium sulfate, and concentrated in vacuo. The amber residue crystallized on standing, and was recrystallized from chloroform/hexanes to provide the *diene* (**1**) as amber crystals (719 mg, 34%): mp 190.5–192 °C; IR ($CHCl_3$) 3015 (s), 2935 (m), 1715 (w), 1610 (m), 1475 (s), 875 (m) cm^{-1}; ^1H NMR (250 MHz, $CDCl_3$) δ 2.95–3.00 (m, 4 H), 3.05–3.10 (m, 4 H), 6.79 (s, 2 H), 7.14–7.28 (comp m, 6 H), 7.53–7.57 (m, 2 H); ^{13}C NMR (69.5 MHz, $CDCl_3$) δ 28.3, 30.1, 116.0, 120.0, 125.3, 126.5, 127.7, 142.0, 143.7, 146.8; λ_{max} (EtOH) 380.8, 361.2, 344.8, 250.0, 204.0 nm (ϵ 28 000, 35 000, 30 000, 13 000, 19 000); chemical ionization mass spectrum, m/e 258.1399 (M^+ calcd for $C_{20}H_{18}$, 258.1408). Anal. Calcd for $C_{20}H_{18}$: C, 92.98; H, 7.02. Found: C, 92.73; H, 6.93.

1-Vinyl-1,2,3,4-tetrahydro-1-naphthol (9).[37] A solution of α-tetralone (**8**, 10.0 g, 68.4 mmol) in 20 mL of benzene was added dropwise over 25 min to a solution of vinylmagnesium bromide (150 mL, 1.0 M in Et_2O, 150 mmol) in 150 mL of benzene. The reaction was stirred for 15 h, after which extractive aqueous workup gave a yellow residue. Flash column chromatography (hexanes:Et_2O, 17:3) afforded the pure *alcohol* (11.8 g, 99%) as a colorless oil: IR ($CHCl_3$) 3595 (m), 3440 (w), 3012 (s), 2945 (s), 1490 (m), 1450 (m), 1440 (m), 995 (m), 945 (m), 926 (m) cm^{-1}; ^1H NMR (250 MHz, $CDCl_3$) δ 1.77–2.03 (m, 5 H), 2.73–2.84 (m, 2 H), 5.20 (dd, J = 1.4, 10.6 Hz, 2 H), 5.29 (dd, J = 1.4, 17.2 Hz, 2 H), 6.04 (dd, J = 10.5, 17.1 Hz, 1 H), 7.08–7.22 (m, 3 H), 7.35–7.40 (m, 1 H); chemical ionization mass spectrum, m/e 174.1054 (M^+ calcd for $C_{12}H_{14}O$, 174.1045).

(*E*)-[2-(1,2,3,4-Tetrahydro-1-naphthylidenyl)ethyl]triphenylphosphonium Bromide (11). Alcohol **9** (6.00 g, 34.4 mmol) in 200 mL of methylene chloride was cooled to 0 °C, and hydrobromic acid (12 mL, 48%) was added all at once with stirring. After 30 min, the reaction was poured into ice–water. The organic layer was isolated and washed with cold, saturated $NaHCO_3$ solution and then brine and subsequently dried ($CaCl_2$). Solvent was removed in vacuo at no higher than room temperature. The bromide was dissolved in 200 mL of benzene and cooled to 5 °C, and triphenylphosphine (9.15 g, 34.9 mmol) was added with stirring. The reaction was allowed to stand at room temperature for 12 h, and then the crystalline product was vacuum-filtered and washed with benzene. The crystals were dried in vacuo, affording the *phosphonium salt* (7.44 g, 43%). Recrystallization from ethanol/benzene provided colorless prisms: mp 160–164 °C; IR ($CHCl_3$) 2940 (s), 1443 (s), 1240 (m), 1113 (s), 689 (s) cm^{-1}; ^1H NMR (250 MHz, $CDCl_3$) δ 1.51 (app quin, J = 6.2 Hz, 2 H), 2.18 (m, 2 H), 2.58 (t, J = 6.1 Hz, 2 H), 4.93 (dd, J = 8.0, 15.4 Hz, 2 H), 5.83–5.91 (m, 1 H), 7.03–7.18 (m, 3 H), 7.32 (d, J = 7.5 Hz, 1 H), 7.57–7.96 (m, 15 H); chemical ionization mass spectrum, m/e 419.1982 (M − Br calcd for $C_{30}H_{28}P$, 418.1929).

(*E*,*E*)-Bis(tetrahydronaphthylidenyl)ethane (2). *n*-Butyllithium (2.32 M in hexanes) was added to a suspension of phosphonium salt **11** (17.57 g, 35.18 mmol) in 200 mL of benzene/THF (1:1) at room temperature under argon until a faint yellow color persisted, and a further 15.15 mL (35.2 mmol) of *n*-butyllithium was added. The resulting suspension was stirred 30 min, after which α-tetralone (**8**, 4.68 mL, 35.2 mmol) was added. The reaction mixture was heated to reflux for 29 h and then allowed to cool. Aqueous extractive workup and flash column chromatography ($CHCl_3$:hexanes, 1:1), followed by crystallization from petroleum ether provided the *diene* (**2**) as bright yellow crystals (4.00 g, 40%): mp 144–146 °C; IR ($CHCl_3$) 3010 (s), 2945 (s) 1484 (s), 1454 (m), 1445 (m), 1230 (m), 1210 (m) cm^{-1}; ^1H NMR (250 MHz, $CDCl_3$) δ 1.89 (app quin, J = 2.5 Hz, 4 H), 2.77–2.82 (m, 8 H), 7.05 (s, 2 H), 7.08–7.23 (m, 6 H), 7.70–7.73 (m, 2 H); ^{13}C NMR (69.5 MHz, $CDCl_3$) δ 23.0, 27.0, 30.7, 119.4, 123.8, 126.1, 126.8, 128.9, 136.1, 136.5, 138.1; λ_{max} (hexanes) 348.8, 247.6, 209.2, 204.4, 201.6, 190.8 nm (ϵ 29 000, 7200, 13 000, 13 000, 14 000, 13 000); chemical ionization mass spectrum, m/e 287.1856 (M + H calcd for $C_{22}H_{23}$, 287.1800). Anal. Calcd for $C_{22}H_{22}$: C, 92.26; H, 7.74. Found: C, 92.29; H, 7.82.

(*E*)- and (*Z*)-(1-Benzosuberanylidenyl)acetic Acid Ethyl Ester (13 and 14). Triethyl phosphonoacetate (28.50 mL, 143.7 mmol) was added dropwise to a suspension of sodium hydride (3.75 g, 80% dispersion in mineral oil, 125 mmol) in 50 mL of benzene over the course of 1 h while the reaction flask was cooled in a water bath. The resulting solution was stirred a further 30 min, after which a solution of 1-benzosuberone (**12**, 20.0 g, 125 mmol) in 35 mL of benzene was added over 5 min. The reaction mixture was heated to reflux for 6 h, then allowed to cool, poured into water, and extracted with ether. Combined extracts were washed with brine, dried over magnesium sulfate, and concentrated in vacuo. Flash column chromatography (hexanes:Et_2O, 19:1 → 9:1) provided the *E*-isomer **13** (6.15 g, 21%) as the first-eluting product and the *Z*-isomer **14** (18.45 g, 64%) as the second-eluting product. Both compounds were obtained as colorless oils. The configuration of the olefin in **13** was established unambiguously by its subsequent conversion to diene **3**, on which an X-ray diffraction structure analysis was performed.

13: IR ($CHCl_3$) 3015 (m), 2990 (m), 2945 (s), 2865 (m), 1710 (s), 1630 (m), 1450 (m), 1375 (s), 1175 (s), 1025 (m), 880 (m) cm^{-1}; ^1H NMR (250 MHz, $CDCl_3$) δ 1.34 (t, J = 7.0 Hz, 3 H), 1.80 (br s, 4 H), 2.76 (br s, 2 H), 3.01 (br s, 4 H), 4.23 (q, J = 7.0 Hz, 2 H), 5.98 (s, 1 H), 7.11–7.27 (comp m, 4 H); chemical ionization mass spectrum, m/e 231.1397 (M + H calcd for $C_{15}H_{19}O_2$, 231.1385).

14: IR ($CHCl_3$) 3015 (m), 2990 (m), 2935 (s), 2860 (m), 1715 (s), 1640 (s), 1450 (s), 1380 (m), 1280 (m), 1215 (s), 1185 (s), 1165 (s), 1105 (m), 1035 (m), 875 (w) cm^{-1}; ^1H NMR (250 MHz, $CDCl_3$) δ 1.07 (t, J = 6.8 Hz, 3 H), 1.78 (br s, 2 H), 1.94 (br s, 2 H), 2.40 (t, J = 5.7 Hz, 2 H), 2.76 (m, 2 H), 3.98 (q, J = 6.8 Hz, 2 H), 5.96 (s, 1 H), 7.02–7.27 (comp m, 4 H); chemical ionization mass spectrum, m/e 231.1402 (M + H calcd for $C_{15}H_{19}O_2$, 231.1385).

(*E*)-2-(1-Benzosuberanylidenyl)ethanol (15). A solution of ester **13** (6.15 g, 26.7 mmol) in 10 mL of diethyl ether was cannulated over 5 min into a stirred suspension of lithium aluminum hydride (1.01 g, 26.6 mmol) in 50 mL of ether at 0 °C under argon. The reaction mixture was stirred at 0 °C for 1 h and then slowly quenched by dropwise addition of water (1 mL), 15% sodium hydroxide solution (1 mL), and finally water (3 mL). After sufficient stirring, a uniform white suspension was achieved. The solid was filtered off and washed with ether. Concentration of the filtrate under reduced pressure gave the *alcohol* (4.93 g, 98%) as a colorless oil: IR ($CHCl_3$) 3610 (m), 3600–3200 (w), 3010 (s), 2940 (s), 2860 (m), 1485 (m), 1450 (m), 1000 (m) cm^{-1}; ^1H NMR (250 MHz, $CDCl_3$) δ 1.37 (t, J = 5.5 Hz, 1 H), 1.72–1.77 (m, 4 H), 2.41 (br s, 2 H), 2.72–2.76 (m, 2 H), 4.35 (t, J = 5.9 Hz, 2 H), 5.66 (t, J = 6.7 Hz, 1 H), 7.06–7.18 (comp m, 4 H); chemical ionization mass spectrum, m/e 188.1187 (M^+ calcd for $C_{13}H_{16}O$, 188.1201). Anal. Calcd for $C_{13}H_{16}O$: C, 82.94; H, 8.57. Found: C, 82.69; H, 8.49.

(*E*)-2-(1-Benzosuberanylidenyl)bromomethane (16). Phosphorus tribromide (1.04 mL, 11.1 mmol) was added dropwise over 5 min to a solution of alcohol **15** (4.93 g, 26.2 mmol) in 100 mL of diethyl ether at room temperature. The reaction mixture was stirred for 30 min and then quenched with excess saturated sodium bicarbonate solution. Extraction with ether, drying of the combined extracts over magnesium sulfate, and evaporation of the solvent in vacuo gave the *bromide* (5.97 g, 91%) as a colorless oil: IR ($CHCl_3$) 3015 (m), 2940 (s), 2860 (m), 1710 (w), 1640 (w), 1485 (m), 1450 (m), 1200 (s), 870 (w) cm^{-1}; ^1H NMR (250 MHz, $CDCl_3$) δ 1.75–1.78 (m, 4 H), 2.48–2.52 (m, 2 H), 2.71–2.75 (m, 2 H), 4.17 (d, J = 8.6 Hz, 2 H), 5.79 (t, J = 8.6 Hz, 1 H), 7.06–7.19 (comp m, 4 H); chemical ionization mass spectrum, m/e 253.0418 (M + H calcd for $C_{13}H_{16}Br$, 253.0416). The bromide was not purified but used directly in the next reaction.

[(*E*)-2-(1-Benzosuberanylidenyl)ethyl]triphenylphosphonium Bromide (17). Triphenylphosphine (15.0 g, 57.2 mmol) was added to a solution of bromide **16** (5.97 g, 23.8 mmol) in 150 mL of benzene at 5 °C under argon. The reaction mixture was allowed to stand at room temperature overnight. The supernatant was removed, and the crystalline product

washed with hot benzene (2 × 20 mL) and dried in vacuo. The colorless crystals of *phosphonium salt* **17** so obtained (14.81 g, 110%) contained benzene by ^{1}H NMR which could not be removed by heating of the sample in vacuo. The salt was used without further purification in the next reaction.

17: mp 85.5–88.5 °C; IR ($CHCl_3$) 2940 (s), 1440 (s), 1240 (s), 1115 (s), 995 (m), 715 (s), 685 (s), 655 (s) cm^{-1}; ^{1}H NMR (250 MHz, $CDCl_3$) δ 1.36–1.38 (m, 2 H), 1.48–1.57 (m, 2 H), 2.17 (br s, 2 H), 2.48–2.53 (m, 2 H), 4.85 (dd, J = 7.7, 15.3 Hz, 2 H), 5.42 (m, 1 H, 6.96–7.23 (comp m, 4 H), 7.66–7.98 (comp m, 15 H); chemical ionization mass spectrum, m/e 433.2015 (M − Br calcd for $C_{31}H_{30}P$, 433.2085).

(*E*,*E*)-Bis(benzosuberanylidenyl)ethane (3). *n*-Butyllithium (1.46 mL, 2.40 M in hexanes, 3.50 mmol) was added to a suspension of phosphonium salt **17** (2.00 g, 3.90 mmol) in 20 mL of benzene/THF (1:1) at 0 °C under argon until a faint yellow color persisted, and a further 1.46 mL (3.50 mmol) was added. The suspension was stirred at room temperature for 45 min, after which 1-benzosuberone (0.56 g, 3.5 mmol) was added. The reaction mixture was heated to reflux for 22 h, then allowed to cool, poured into water, and extracted with ether. Combined organic extracts were washed with brine, dried over magnesium sulfate, and concentrated in vacuo. Flash column chromatography (hexanes:$CHCl_3$, 1:1) followed by crystallization from methylene chloride/hexanes gave the *diene* (**3**) as colorless prisms (144 mg, 13%): mp 186.5–187.5 °C; IR ($CHCl_3$) 3065 (w), 3010 (m), 2935 (s), 2855 (m), 1705 (w), 1600 (w), 1480 (m), 1450 (m), 890 (w) cm^{-1}; ^{1}H NMR (250 MHz, $CDCl_3$) δ 1.74–1.76 (m, 8H) 2.58 (br s, 4 H), 2.76–2.78 (m, 4 H), 6.43 (s, 2 H), 7.09–7.28 (comp m, 8 H); ^{13}C NMR (69.5 MHz, $CDCl_3$) δ 27.0, 27.6, 29.6, 34.8, 123.5, 126.2, 126.9, 127.6, 128.8, 139.9, 144.6, 145.2; λ_{max} (hexanes) 292.4 and 202.0 nm (ϵ 27 000 and 25 000); chemical ionization mass spectrum, m/e 315.2110 (M + H calcd for $C_{24}H_{27}$, 315.2113). Anal. Calcd for $C_{24}H_{26}$: C, 91.67; H, 8.33. Found: C, 91.48; H, 8.20.

Acknowledgment. This research was supported by the National Science Foundation—Laboratory for Research on the Structure of Matter (LRSM), Grant No. DMR-85-19059, and in part by grants to R.M.H. and A.B.S. from NSF and NIH. In addition, we thank Drs. G. Furst, J. Dykins, and P. Carroll, Directors of the University of Pennsylvania Spectroscopic Facilities, for aid in obtaining respectively the high-field NMR, high-resolution mass spectral, and X-ray crystallographic data and Wing Sau Young for determining the UV spectral data.

Core and Valence-Shell Electronic Excitation of Nickel Tetracarbonyl by High-Resolution Electron Energy Loss Spectroscopy

Glyn Cooper, Kong Hung Sze, and C. E. Brion*

Contribution from the Department of Chemistry, University of British Columbia, Vancouver, B.C., Canada V6T 1Y6. *Received September 30, 1988*

Abstract: Core (inner-shell) and valence-shell electron energy loss spectra of $Ni(CO)_4$ are compared with corresponding spectra of free CO under kinematic conditions where the spectra are dominated by dipole-allowed transitions. The inner-shell spectra encompass the C 1s, O 1s, and Ni 3p excitation and ionization regions of $Ni(CO)_4$. The C and O 1s spectra of $Ni(CO)_4$ show some major similarities to those of free CO. In particular both the C 1s and the O 1s inner-shell spectra of both molecules exhibit intense 1s → π^* and 1s → σ^* transitions. For the case of the C 1s → π^* transitions vibrational structure is resolved for both $Ni(CO)_4$ and CO. There are also significant differences, however, which are related to the different manifolds of final states available in the two molecules. Tentative assignments are suggested for the $Ni(CO)_4$ spectra using molecular orbital energy level and term value considerations. The implications of the results for studying dπ → pπ back-bonding in transition-metal carbonyl complexes are discussed.

Transition-metal carbonyl complexes have been the subject of a large amount of spectroscopic measurement[1-15] and theoretical investigation[2,7,13,16-26] due to their high photochemical and catalytic activity.[27-32] They have been used as prototype models for the bonding of CO to transition-metal surfaces[10,33-35] and serve as model systems for many organometallic complexes. An understanding of the electronic structures of transition-metal carbonyl complexes is thus of great importance to diverse areas of practical importance.

Although $Ni(CO)_4$ is the simplest example of the tetrahedral metal carbonyl species, its valence-shell photoabsorption spectrum has received little attention, and to date no core excitation spectra

(1) Reutt, J. E.; Wang, L. S.; Lee, Y. T.; Shirley, D. A. *Chem. Phys. Lett.* **1986**, *126*, 399.
(2) Hillier, I. H.; Guest, M. F.; Higginson, B. R.; Lloyd, D. R. *Mol. Phys.* **1974**, *27*, 215.
(3) Chen, H. W.; Jolly, W. L. *Inorg. Chem.* **1979**, *18*, 2548.
(4) Chambers, S. A. Ph.D. Thesis, Oregon State University, 1978.
(5) Bancroft, G. M.; Boyd, B. D.; Creber, D. K. *Inorg. Chem.* **1978**, *17*, 1008.
(6) Lever, A. B. P.; Ozin, G. A.; Hanlan, A. J. L.; Power, W. J.; Gray, H. B. *Inorg. Chem.* **1979**, *18*, 2088.
(7) Schreiner, A. F.; Brown, T. L. *J. Am. Chem. Soc.* **1968**, *90*, 3366.
(8) Koerting, C. F.; Walzl, K. N.; Kupperman, A. *J. Chem. Phys.* **1987**, *86*, 6646.
(9) Cooper, G.; Green, J. C.; Payne, M. P.; Dobson, B. R.; Hillier, I. H. *J. Am. Chem. Soc.* **1987**, *109*, 3836.
(10) Plummer, E. W.; Salaneck, W. R.; Miller, J. S. *Phys. Rev. B* **1978**, *18*, 1673.
(11) Loubriel, G.; Plummer, E. W. *Chem. Phys. Lett.* **1979**, *64*, 234.
(12) Chastain, S. K.; Mason, R. W. *Inorg. Chem.* **1981**, *20*, 1395.
(13) Beach, N. A.; Gray, H. B. *J. Am. Chem. Soc.* **1968**, *90*, 5713.
(14) Iverson, A.; Russell, B. R. *Chem. Phys. Lett.* **1970**, *6*, 307.
(15) Tossell, J. A.; Moore, J. H.; Olthoff, K. *J. Am. Chem. Soc.* **1984**, *106*, 823.
(16) Hillier, I. H.; Saunders, V. R. *Mol. Phys.* **1971**, *22*, 1025.
(17) Loubriel, G. *Phys. Rev. B* **1979**, *20*, 5339.
(18) Rosch, N.; Jorg, H.; Kotzian, M. *J. Chem. Phys.* **1987**, *86*, 4038.
(19) Baerends, E. J.; Ros, P. *Mol. Phys.* **1975**, *30*, 1735.
(20) Ford, P. C.; Hillier, I. H. *J. Chem. Phys.* **1983**, *80*, 5664.
(21) Yang, C. Y.; Arratia-Perez, R.; Lopez, J. P. *Chem. Phys. Lett.* **1984**, *107*, 112.
(22) Dick, B.; Freund, H.-J.; Hohlneicher, G. *Mol. Phys.* **1982**, *45*, 427.
(23) Johnson, J. B.; Klemperer, W. G. *J. Am. Chem. Soc.* **1977**, *99*, 7132.
(24) Sherwood, D. E.; Hall, M. B. *Inorg. Chem.* **1980**, *19*, 1905.
(25) Bursten, B. E.; Freier, B. G.; Fenske, R. F. *Inorg. Chem.* **1980**, *19*, 1810.
(26) Bauschlicher, Jr., C. W.; Bagus, P. S. *J. Chem. Phys.* **1984**, *81*, 5889.
(27) Wrighton, M.; Hammond, G. S.; Gray, H. B. *J. Organomet. Chem.* **1974**, *70*, 283.
(28) Koerner van Gustorf, E.; Guerals, F. W. *Fortsch. Chem. Forsch.* **1969**, *13*, 366.
(29) Lewandos, G. S.; Pettit, R. *J. Am. Chem. Soc.* **1971**, *93*, 7087.
(30) Leigh, G. L.; Fischer, E. O. *J. Organomet. Chem.* **1965**, *4*, 461.
(31) Fischer, E. O.; Fritz, H. P. *Angew. Chem.* **1961**, *73*, 353.
(32) Wrighton, M. *Chem. Rev.* **1974**, *74*, 401, and references therein.
(33) Muetterties, E. *Science* **1976**, *194*, 1150.
(34) Muetterties, E. *Science* **1977**, *196*, 839.
(35) Fruend, H.-J.; Plummer, E. W. *Phys. Rev. B* **1981**, *23*, 4859.

0002-7863/89/1511-5051$01.50/0